ISBN: 978-3-95450-227-1 ISSN: 2673-5490 doi:10.18429/JACoW-IPAC2022-MOPOPT019

WAKEFIELD STUDIES FOR A BUNCH ARRIVAL-TIME MONITOR CONCEPT WITH ROD-SHAPED PICKUPS ON A PRINTED CIRCUIT BOARD FOR X-RAY FREE-ELECTRON LASERS*

B. E. J. Scheible[1]†, A. Penirschke, Technische Hochschule Mittelhessen, Friedberg, Germany
M. K. Czwalinna, H. Schlarb, Deutsches Elektronen-Synchrotron DESY, Hamburg, Germany
W. Ackermann, H. De Gersem, Technische Universität Darmstadt, Darmstadt, Germany
[1]also at Technische Universität Darmstadt, Darmstadt, Germany

Abstract

The European XFEL (EuXFEL) and other notable X-ray Free-Electron Laser facilities rely on an all-optical synchronization system with electro-optical bunch arrival-time monitors (BAM). The current BAMs were benchmarked with a resolution of 3.5 fs for nominal 250 pC bunches at the EuXFEL, including jitter of the optical reference system. The bunch arrival-time jitter was reduced to about 5 fs with a beam-based feedback system. For future experiments at the EuXFEL the bunch charge will be decreased to a level where the existing system's accuracy will no longer be sufficient. In simulations a concept based on rod-shaped pickups mounted on a printed circuit board indicated its potential for such low charge applications. For the feasibility of the proposed design, its contribution to the total impedance is essential. In this work the design and an intermediate version are compared to state-of-the-art BAM regarding their wake potential. Furthermore, measures to mitigate wakefields are discussed.

INTRODUCTION

X-ray Free-Electron Lasers (XFELs) are 4th generation light sources for experiments with high temporal and spatial resolution [1]. A major challenge in utilizing the XFEL's full potential is fs-precision synchronization of subsystems in a several km-long facility [2]. The synchronization includes high-precision arrival-time measurements [3].

Sufficient precision can be achieved by an all-optical synchronization system [3, 4], which contains bunch arrival-time monitors (BAMs) with the electro-optical (eo) detection scheme described in [4]. They provide non-destructive measurements of individual bunch arrival times with high precision. The European XFEL (EuXFEL) [3] recently reported an eo-BAM resolution of 3.5 fs at nominal 250 pC [5] with cone-shaped pickups [6].

In order to reach single-digit fs measurement resolution below 20 pC, the BAMs have to be improved. A proposed design will potentially extract a voltage signal ten times higher as the current pickups [7].

Since some of the beam energy is extracted, the invasiveness due to wakefield should be evaulated. Bunch-to-bunch and short-range interaction might be problematic in the updated pickup, because of the sharp edges in the cross-section. Additionally striving for higher signal intensity will also extract more energy. Therefore, it is necessary to check the wake potential while evaluating the design options.

Wakefields

Wakefields emerge from interaction between a charged particle and its surroundings [8]. Finite conductivity and geometric changes in the beam pipe are sources of wakefields [8, 9], which affect source and trailing particles [8].

The wake function describes the response to a pulse excitation [10], which, separated by orientation, is‡

$$w_\nu\left(\vec{r}_0, \vec{r}, z\right) = \frac{1}{q_0 q} \int_{-\infty}^{\infty} \vec{F}_\mathrm{L}\left(\vec{r}_0, s, \vec{r}, z\right) \cdot \vec{e}_\nu \mathrm{d}s\,, \qquad (1)$$

where ν is either $\|$, x or y and $\vec{e}_\nu$ the corresponding standard basis vector in $\mathbb{R}^3$. $\vec{r}_0$, q_0 and $\vec{r}$, q are transverse position and charge of source respectively test particle, z is the longitudinal distance between them, s the trajectory and $\vec{F}_\mathrm{L}$ the Lorentz force [8, 9]. Sometimes it is convenient to use the Fourier transform, called wake impedance Z_ν [8].

The effect on a test charge by wakefields of the entire bunch is defined as the convolution of the bunch's linear charge distribution $\lambda(z)$ and the wake function normalized to the bunch charge Q_B [10]. For longitudinal wakes this is

$$W_\|(z) = \frac{1}{Q_\mathrm{B}} \int_{-\infty}^{\infty} w_\|\left(z' - z\right) \lambda\left(z'\right) \mathrm{d}z'\,. \qquad (2)$$

The total wake loss factor (WLF) [11–13], which is the energy lost by the bunch per squared charge, is‡

$$k_\sigma = \frac{\Delta E}{Q_\mathrm{B}^2} = -\frac{1}{Q_\mathrm{B}} \int_{-\infty}^{\infty} \lambda\left(z\right) W_\|\left(z\right) \mathrm{d}z\,. \qquad (3)$$

The rms energy spread per charge [12], referred to as energy spread factor (ESF), is calculated by‡

$$ESF\left(\sigma\right) = \sqrt{\frac{1}{Q_\mathrm{B}} \int_{-\infty}^{\infty} \lambda\left(z\right) \left[W_\|\left(z\right) + k_\sigma\right]^2 \mathrm{d}z}\,. \qquad (4)$$

Numerical Field Calculation

In this work the wakefield solver of CST Particle Studio® (PS) was applied with integration method "Indirect Interfaces", at least 300 mm simulated wakelength and a Gaussian excitation. CST PS uses the finite integration technique

* Work supported by the German Federal Ministry of Education and Research (BMBF) under contract No. 05K19RO1.

† bernhard.scheible@iem.thm.de

‡ It is common to add a minus sign in the longitudinal wake function to associate energy loss with a positive value. The (total) WLF in Eq. (3) then also has an opposite sign, e.g. in [11,12]. Likewise the sign in Eq. (4) would switch. In this work we follow the definition used by CST® [13].

ISBN: 978-3-95450-227-1 ISSN: 2673-5490 doi:10.18429/JACoW-IPAC2022-MOPOPT019

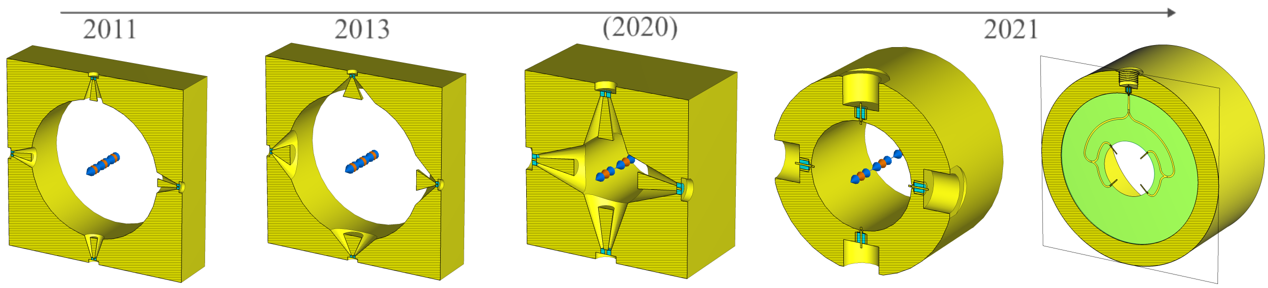

(a) 1st Generation [6], $R_{\mathrm{BL}} = 20.25\,\mathrm{mm}$
(b) 2nd Generation [6], $R_{\mathrm{BL}} = 20.25\,\mathrm{mm}$
(c) Scaled 1st Gen. [19], $R_{\mathrm{BL}} = 5.0\,\mathrm{mm}$
(d) Demonstrator [7], $R_{\mathrm{BL}} = 7.5\,\mathrm{mm}$
(e) rPCB-BAM from [7], $R_{\mathrm{BL}} = 20.25\,\mathrm{mm}$

Figure 1: Designs used for wakefield analysis. The parameter can be found in the corresponding publications.

in time domain [11, 13]. The longitudinal wake potential is found by integration of the longitudinal electrical fields along a straight path, the transverse counterpart with the Panovsky-Wenzel theorem [14] and the wake impedance by a single sided discrete Fourier transform [11, 13].

It is impossible to extract the wake function from the numerical wake potential and it is not feasible to allocate the computing power necessary to calculate sub-mm bunches in an early stage. Nonetheless in an investigation at SPEAR II the total WLF followed a power-law by the power of −1.41 [15]. Because the power depends on the wake impedance and thus the structure's geometry, the total WLF found by simulation was fitted with the general power law

$$k_{\sigma}\left(\sigma_{z}\right) = \hat{K} \cdot \left(\frac{\sigma_{z}}{1\,\mathrm{mm}}\right)^{-\alpha} + k_{\infty}\,. \tag{5}$$

This function can be used to extrapolate the WLF towards sub-mm bunches as in [16, 17]. However, exceeding one order of magnitude between simulated bunch and real bunches leads to a significant prediction uncertainty.

RESULTS

Simulations were carried out for different pickup structures. As a reference two established high-bandwidth cone-shaped pickups, defined in [6], are used. The small cone (Fig. 1a) is referred to as 1st, the large (Fig. 1b) as 2nd generation (gen.). They are accompanied by a design with beamline radius $R_{\mathrm{BL}} = 5\,\mathrm{mm}$ (Fig. 1c), chosen to scale to the minimum diameter found in the EuXFEL. Furthermore, this is in the range of the 8 mm and 16 mm lines at SwissFEL, also equipped with cone-shaped pickups [18]. The 3rd design (Fig. 1d) represents the non-hermetic demonstrator of an open-coaxial pickup presented in [7]. The 4th pickup structure (Fig. 1e), also introduced in [7], combines rod-like pickups with a printed circuit board (PCB) combination network and is referred to as the rPCB design.

Long-Range Wakefields

In the scaled 1st gen. pickups a long-range wake was found. Figure 2 (top) shows the wake potential caused by a 1 mm bunch. About 5 cm behind the bunch center a distinct sinusoidal form is visible. The wake impedance, pictured in Fig. 2 (bottom), has a pronounced peak at 21.9 GHz.

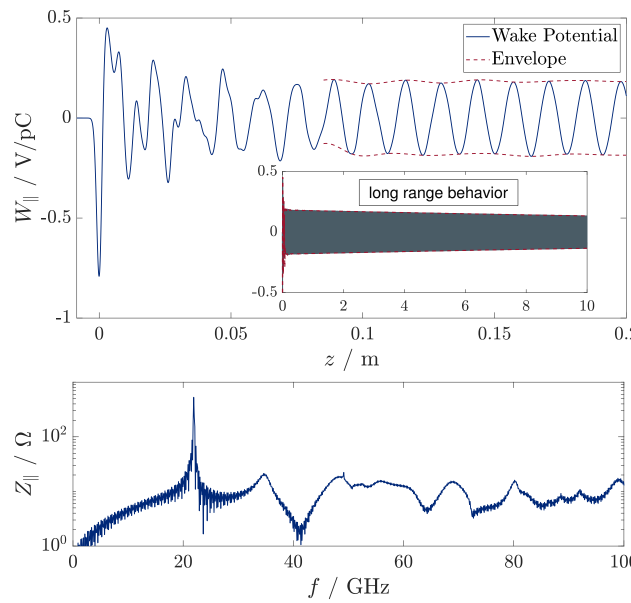

Figure 2: Simulated $W_{\parallel}$ (top) and $Z_{\parallel}$ (bottom) of the 1st gen. pickups with $R_{\mathrm{BL}} = 5\,\mathrm{mm}$. The simulation was executed with 1 pC, 1 mm bunch and 10 m wakelength.

Evaluation of the electromagnetic fields in time domain revealed a TM_{10} mode stationary between the pickups. In the beamline the TM_{10} mode can propagate above cutoff frequency ω_{c}, which is 22.9 GHz. Therefore the long-range wake is attributed to a trapped mode as described in [20]. In this phenomena a discontinuity on the beam wall lowers the resonance frequency and prevents the mode from propagating [11, 20, 21].

The amplitude in Fig. 2 (top) follows an exponential decay with relaxation length $l_{\mathrm{r}} = 32.227(1)\,\mathrm{m}$, which is about half the minimum bunch spacing at the EuXFEL, possibly leaving more than 10 % of the amplitude at arrival of the next bunch. The estimation for wall losses

$$l_{\mathrm{r}} = c_0 \tau \approx \frac{2 c_0 R_{\mathrm{BL}}}{\omega_{\mathrm{c}} \delta_{\mathrm{s}}}\,, \tag{6}$$

with skin depth δ_{s} [11, 22], is about 50 % higher. This indicates that a third of the energy is dissipated through other loss channels. Because the electric field of an ideal

ISBN: 978-3-95450-227-1 ISSN: 2673-5490 doi:10.18429/JACoW-IPAC2022-MOPOPT019

Table 1: Fit Parameter and Resulting WLF at 1 mm and 180 fs According to Eq. (5), see also Fig. 3

	adj. R²	**α**	**k_∞ in V/pC**	**$k_{1\,\mathrm{mm}}$ in V/pC**	**$k_{180\,\mathrm{fs}}$ in V/pC**	**$\mathrm{PI}_{99\,\%}(k_{180\,\mathrm{fs}})$ in V/pC**	
rPCB	1.000	0.97 (0.96 to 0.99)	−1.163	9.665	185.07	180.17	189.98
scaled G1	0.998	1.33 (1.11 to 1.55)	−0.069	0.483	26.79	12.21	41.37
2nd gen.	1.000	1.03 (0.98 to 1.07)	−0.019	0.132	3.02	2.72	3.31
1st gen.	0.997	1.17 (0.95 to 1.39)	−0.006	0.027	0.98	0.52	1.44
Demon.	0.999	2.73 (2.54 to 2.92)	0.000	0.004	11.24	6.55	15.93

TM_{10} mode is tangential and vanishing at the pickup surface, these wakes will not substantially affect the retrieved signal, but potentially subsequent bunches. Trapped modes may occur in cone-shaped pickups, which act as a hole/bulge, but not in irises [20].

Total Wake Loss Factor

Figure 3 shows a comparison of the total WLF as function of the bunch length. The graph is linearized as log-log plot of k_σ minus an individual constant k_∞ from the resulting fit parameters in Table 1. The fit is shown by solid lines and simulation results by symbols. Dashed lines correspond to the 99 % prediction intervals (PI). Extrapolated sub-mm values are also summarized in Table 1.

The 1st gen. pickups follow a power of −1.17 to 1.33, which is less sensitive to the bunch length than resistive walls ($\alpha \approx -1.5$ [11]). The first design generations have a single digit WLF with a 180 fs bunch, but scaling of the beampipe increases it to $k^{\mathrm{scG1}}_{180\,\mathrm{fs}} = 26.79\ (12.21\ \text{to}\ 41.37)\ \mathrm{V\,pC^{-1}}$.

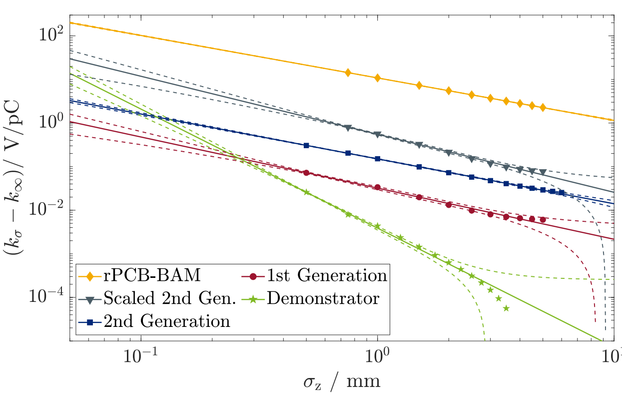

Figure 3: Log-log plot of the total WLF as a function of bunch length for different geometries. Symbols indicate CST® simulation results, solid lines a power law fit and dashed lines are the 99 % PI.

The open-coax demonstrator is most sensitive to the bunch length, with a power of −2.73, comparable to the −3 of a low Q cavity [11]. This leads to a WLF in between the cone-shaped designs for short bunches, though the demonstrator undercuts them by more than one order in the mm range.

The rPCB design follows a power of −0.97. This matches the power of −1 for a collimator/iris [11]. Additionally the analytical WLF in [11] gives about $10\ \mathrm{V\,pC^{-1}}$ with $\sigma_z = 1$ mm, comparable to the $9.7\ \mathrm{V\,pC^{-1}}$ found by simulation. This strongly implies that the design can be treated as collimator/iris from wakefield point of view. The energy lost by the short 1 pC-bunch is about 1.2 GeV. For the much longer 1 mm-bunch an ESF of $4.15\ \mathrm{V\,pC^{-1}}$ is found with the trapezoidal integration function of MATLAB®.

Similar to the rPCB the 2nd gen. pickup follows a power of −1.03. Protruding cones could also act like an iris.

Mitigation of Wakefields

The rPCB design gave the best signal in earlier studies [7] but is disadvantageous from wakefield perspective. Because of its low extension one may think of integrating the rPCB into existing structures, e.g. a collimator, to not substantially add to the wake budget and to provide additional shielding. However there the β function will be high and therefore, incident of electrons, radiation as well as space limitation and movable parts probably will prevent this option. Furthermore, it is considered to taper both sides of the flat PCB structure or to use a quasi-coaxial transmission line with via-holes in the PCB. The later reduces signal noise and by additional removal of excess parts in the PCB could reduce the WLF by nearly 40 % as preliminary simulations showed.

CONCLUSION

A cone-shaped approach, which is already used in many facilities, has a low wake potential. For a considerably long bunch the demonstrator in [7] causes even less wakefields but it is sensitive to the bunch length. Furthermore, effects by transition to smaller diameters for scaled BAM and demonstrator are missing in this analysis.

Designs with notches in the wall, introduced by cone-shaped or open-coax pickups, can house trapped modes, as observed for the 1st gen. BAM with $R_{\mathrm{BL}} = 5$ mm. These modes can be dangerous for subsequent bunches.

New designs optimize the signal slope for higher arrival-time resolution. Wakefields have not been considered in previous works. The new rPCB structure has a significant larger wake loss factor, approximately two orders in magnitude, but it is still in the range of other accelerator components installed in XFEL. Careful positioning in the beamline or integration into other systems may improve the measurement and shield the BAM from beam incident while reducing the additional wake load. This is also possible by reducing the transverse cross-section of the PCB.

ISBN: 978-3-95450-227-1 ISSN: 2673-5490 doi:10.18429/JACoW-IPAC2022-MOPOPT019

REFERENCES

[1] E. J. Jaeschke, S. Khan, J. R. Schneider, and J. B. Hastings, "Synchrotron light sources and free-electron lasers: Accelerator physics, instrumentation and science applications", 2nd Edition, Cham: Springer International Publishing, 2020. doi:10.1007/978-3-030-23201-6

[2] S. Schulz *et al.*, "Femtosecond all-optical synchronization of an X-ray free-electron laser", *Nat. Commun.*, vol. 6, p. 5938, 2015. doi:/10.1038/ncomms6938

[3] T. Lamb *et al.*, "Large-Scale Optical Synchronization System of the European XFEL with Femtosecond Precision", in *Proc. IPAC'19*, Melbourne, Australia, May 2019, pp. 3835–3838. doi:10.18429/JACoW-IPAC2019-THPRB018

[4] F. Löhl *et al.*, "Electron bunch timing with femtosecond precision in a superconducting free-electron laser", *Phys. Rev. Lett.*, vol. 104, no. 14, p. 144801, Apr. 2010. doi:10.1103/PhysRevLett.104.144801

[5] M. K. Czwalinna *et al.*, "Beam arrival stability at the European XFEL", in *Proc. IPAC'21*, Campinas, Brazil, May 2021, pp. 3714–3719. doi:10.18429/JACoW-IPAC2021-THXB02

[6] A. Angelovski *et al.*, "Pickup Signal Improvement for High Bandwidth BAMs for FLASH and European - XFEL", in *Proc. IBIC'13*, Oxford, UK, Sep. 2013, paper WEPC40, pp. 778–781.

[7] B. E. J. Scheible *et al.*, "Bunch arrival-time measurement with rod-shaped pickups on a printed circuit board for X-ray free-electron lasers", in *Proc. IBIC'21*, Pohang, Korea, Sep. 2021, pp. 417-420. doi:10.18429/JACoW-IBIC2021-WEPP19

[8] H. Wiedemann, *Particle Accelerator Physics*. Cham: Springer International Publishing, 2015. doi:10.1007/978-3-319-18317-6

[9] S. Myers and H. Schopper, *Particle Physics Reference Library: Volume 3: Accelerators and Colliders*", 4th Ed. Cham: Springer International Publishing, 2020. doi:10.1007/978-3-030-34245-6

[10] C. Zannini, "Electromagnetic Simulation of CERN Accelerator Components and Experimental Applications", Ph.D. thesis, Laboratoire de Physique des Accélérateurs de Particules, École Polytechnique Fédérale de Lausanne, Switzerland, 2013.

[11] A. W. Chao, *Handbook of Accelerator Physics and Engineering*, 2nd Ed. Singapore: World Scientific Publishing Co Pte Ltd, 2013. isbn:9814415855

[12] A. Novokhatski, M. Timm, and T. Weiland, "Single Bunch Energy Spread in the TESLA Cryomodule: tesla1999-16", Tesla Collaboration, Rep. TESLA 99-16, Sept. 1999.

[13] CST Online Help 2020, hosted by the Massachusetts Institute of Technology. http://space.mit.edu/RADIO/CST_online/cst_studio_suite_help.htm

[14] W. K. H. Panofsky and W. A. Wenzel, "Some considerations concerning the transverse deflection of charged particles in radio-frequency fields", *Rev. Sci. Instrum.*, vol. 27, no. 11, p. 967, 1956. doi:10.1063/1.1715427

[15] P. B. Wilson *et al.*, "Bunch lengthening and related effects in SPEAR II", *IEEE Transactions on Nuclear Science*, vol. 24, no. 3, pp. 1211-1214, 1977. doi:10.1109/TNS.1977.4328899

[16] H.-W. Glock, M. Abo-Bakr, J. Kolbe, F. Pflocksch, A. Schaelicke, and C. Potratz, "Loss factor and impedance analysis of warm components of BERLinPro", in *Proc. IPAC'15*, Richmond, VA, USA, May 2015, pp. 128–131. doi:10.18429/JACoW-IPAC2015-MOPWA018

[17] M. H. Awida, P. Berrutti, T. N. Khabiboulline, A. Saini, and V. P. Yakovlev, "Wakefield loss analysis of the elliptical 3.9 GHz third harmonic cavity", in *Proc. NAPAC'13*, Pasadena, CA, USA, Sep.-Oct. 2013, paper WEPAC32, pp. 847–849.

[18] V. R. Arsov *et al.*, "First results from the bunch arrival-time monitors at SwissFEL", in *Proc. IBIC'18*, Shanghai, China, Sep. 2018, pp. 420–424. doi:10.18429/JACoW-IBIC2018-WEPA20

[19] B. E. J. Scheible, W. Ackermann, M. K. Czwalinna, H. De Gersem, A. Penirschke, and H. Schlarb, "Evaluation of a novel pickup concept for ultra-low charged short bunches in X-ray free-electron lasers", in *Proc. IBIC'20*, Santos, Brazil, Sep. 2020, pp. 145–149. doi:10.18429/JACoW-IBIC2020-WEPP21

[20] G. V. Stupakov and S. S. Kurennoy, "Trapped electromagnetic modes in a waveguide with a small discontinuity", *Phys. Rev. E: Stat. Phys. Plasmas Fluids Relat. Interdiscip. Top.*, vol. 49, no. 1, pp. 794-799, 1994. doi:10.1103/PhysRevE.49.794

[21] R. Schuhmann and T. Weiland, "Rigorous analysis of trapped modes in accelerating cavities", *Phys. Rev. Spec. Top. Accel Beams*, vol. 3, no. 12, 2000. doi:10.1103/PhysRevSTAB.3.122002

[22] S. S. Kurennoy, "Trapped modes in waveguides with many small discontinuities", *Phys. Rev. E: Stat. Phys. Plasmas Fluids Relat. Interdiscip. Top.*, vol. 51, no. 3, pp. 2498–2509, 1995. doi:10.1103/PhysRevE.51.2498